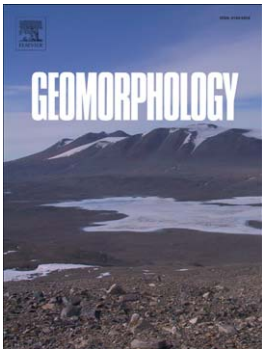

Development and recent activity of the San Andrés landslide on El Hierro, Canary Islands, Spain

Jan Klimeš, Jorge Yepes, Laura Becerril, Michal Kusák, Inés Galindo, Jan Blahut

PII: S0169-555X(16)30052-6
DOI: doi: 10.1016/j.geomorph.2016.02.018
Reference: GEOMOR 5519

To appear in: *Geomorphology*

Received date: 18 November 2014
Revised date: 19 January 2016
Accepted date: 18 February 2016

Please cite this article as: Klimeš, Jan, Yepes, Jorge, Becerril, Laura, Kusák, Michal, Galindo, Inés, Blahut, Jan, Development and recent activity of the San Andrés landslide on El Hierro, Canary Islands, Spain, *Geomorphology* (2016), doi: 10.1016/j.geomorph.2016.02.018

Development and recent activity of the San Andrés landslide on El Hierro, Canary Islands, Spain

Jan Klimeš[a*], Jorge Yepes[b], Laura Becerril[c], Michal Kusák[d, a], Inés Galindo[e], Jan Blahut[a]

[a] Institute of Rock Structure and Mechanics, Czech Academy of Sciences, V Holešovičkách 41, 182 09, Prague 8, Czech Republic

[b] University of Las Palmas de Gran Canaria, Department of Civil Engineering-IOCAG, C/Juan de Quesada 30, Las Palmas de Gran Canaria, 35001, Spain

[c] Institute of Earth Sciences Jaume Almera, ICTJA-CSIC, Lluis Sole i Sabaris s/n, 08028, Barcelona, Spain

[d] Charles University in Prague, Faculty of Science, Department of Physical Geography and Geoecology, Albertov 6, 128 43, Prague 2, Czech Republic

[e] Spanish Geological Survey (IGME), Unit of Canary Islands, Alonso Alvarado, 43, 2ºA, Las Palmas de Gran Canaria, 35003, Spain

*Corresponding author:

Jan Klimeš

tel.: +420723349886

Email address: klimes@irsm.cas.cz

Abstract

Extremely voluminous landslides with a long run-out (also known as megalandslides) on oceanic volcanic islands are infrequent denudational processes on such islands. At the same time, they represent a major geological hazard that must be looked into to avoid negative consequences for the inhabitants of these islands. Their occurrence can be related to periods of intense seismo-volcanic activity, similar to that which occurred on El Hierro Island over 2011-2012. Landslides on volcanic islands are studied using onshore and offshore geological, geophysical and geomorphological records, considering their unique triggering conditions (e.g. lava intrusions, eruptive vents, magma chamber collapses). Previous work has pointed out similarities between specific cases of landslides on volcanic islands and deep-seated gravitational slope deformations (DSGSDs) which are typical in high mountain settings. Nevertheless, the methodological approaches and concepts used to investigate DSGSDs are not commonly applied on volcanic islands studies, even though their use may provide new information about the development stage, recent movements and future hazards. Therefore, this approach for studying the San Andrés landslide (SAL) on El Hierro (Canary Islands) has been developed applying a detailed morphological field mapping, an interpretation of digital elevation models, structural measurements, kinematic testing, and a precise movement monitoring system. The acquired information revealed a strong structural influence on the landslide morphology and the presence of sets of weakened plains acting as the sliding surfaces of the SAL or secondary landslides within its body. The presence of secondary landslides, deep erosive gullies, coastal cliffs and high on-shore relative relief also suggests a high susceptibility to future landslide movement. Direct monitoring on the landslide scarps and the slip plane, performed between February 2013 and July 2014, using an automated optical-mechanical crack gauge with a precision of up to 10^{-2} mm, detected creep movement in the order of 1 mm yr^{-1} with a persistent sinistral component as well as episodic horizontal

and a subtle vertical movement. This monitoring will continue in the future in order to verify the initial observations, which instead of long-term movement patterns, could represent a landslide response to the period of an intense seismo-volcanic activity during 2011-12.

Key words: deep-seated gravitational slope deformations (DSGSDs); landslide monitoring; creep movements; Canary Islands

1. Introduction

Large and extremely voluminous coastal and submarine landslides (up to 10^4 km^3, Whelan and Kelletat, 2003) with run-out often exceeding tens of kilometres, as well as deposits below the sea level, are commonly referred to as megalandslides. These megalandslides are an inherent part of volcanic islands development. They have been widely reported from volcanic islands such as Hawaii, Reunion, Madeira, Azores, Cape Verde, Stromboli and the Canary Islands (Moore et al., 1995; Labazuy, 1996; Tibaldi, 2001, 2004; Masson et al., 2008; Mitchell et al., 2012; Carracedo, 2014). Megalandslide is a non-genetic term that covers different landslide types and it resembles the term deep-seated gravitational slope deformations (DSGSDs) used for large, mountain-scale, subaerial landslides. DSGSDs are further characterized by the development of specific morphological forms (e.g. scarps, antithetic scarps, double-crest ridges, trenches); absence of well-defined shear surfaces and creep movements that often evolve using existing structures (e.g. faults, fold axes, bedding planes; Dramis and Sorriso-Valvo, 1994; Agliardi et al., 2001) creating favourable conditions for secondary landslide development (Cimarelli and De Rita, 2010). DSGSDs are several kilometers long and hundreds of meters thick, with conditions suitable for future slope failure development (Crosta et al., 2014; Jargon et al. 2014). A large number of DSGSDs has been identified, described and monitored in a variety conditions, providing detailed information

about their circumstances of occurrence, and triggering factors. In particular, Cimarelli and De Rita (2010) showed that many morphological features affecting megalandslides on volcanic islands are similar to those described as associated with DSGSDs.

Investigation of megalandslides on volcanic islands is difficult compared to subaerial DSGSDs on continents as the megalandslides have relatively low abundance, have most of their landslide body below the sea level and, in most cases, the catastrophic movements destroyed onshore evidence of the megalandslides development (Day et al., 1997). All the above forces scientists to investigate this phenomenon using geological and geophysical methods applied mostly at small scales (Gee et al., 2001; Masson et al., 2002) which hamper determination of hazard levels for the whole landslide. This is the case of the Canary Islands where large landslides are considered a major geological hazard (Krastel et al., 2001). Their hazard is being broadly recognized mainly during periods of intense seismic and volcanic activity (López et al., 2012). Recently, a period of submarine eruption accompanied by intense seismicity (Las Calmas Sea submarine eruption) hit El Hierro in 2011-2012 (López et al., 2012). This island hosts, among other megalandslides, the San Andrés Landslide (SAL) which offers a rare opportunity to study geological conditions and recent movement activity of a partly failed megalandslide (Day et al, 1997; Gee et al., 2001). Previous research of the SAL (Carracedo et al., 2001; Becerril et al., 2015) pointed out the existence of prominent morphological features: scarps and antithetic scarps, which match DSGSDs diagnostic landforms. Nevertheless, no detailed structural and morphological investigations or representative and precise monitoring of possible landslide movements have been done so far. Therefore, we have investigated, in depth, its subaerial morphology, structural conditions and established a long-term monitoring network to detect potential precursory deformations of possible future increased movement rates of the landslide. Here we present more than one year of monitoring results and information about the SAL limits, its morphology, structural

settings and occurrence pattern of secondary landslides on the SAL. This new evidence allows initial assumptions about the dynamics of its recent movements and re-examination of its development stage as basis for a landslide hazard assessment.

2. Controlling factors of landslide occurrence on the Canary Islands

The occurrence of megalandslides on the Canary Islands, including El Hierro, has been related to triggering factors that act over relatively short time periods. The majority is related to volcanic activity and other processes represented by the intrusion of dykes (Day et al., 1997; Krastel et al., 2001; Masson et al., 2002), which is associated with changes in fluid pore pressure (Moore et al., 1994; Voight, 2000) or seismicity (Gee et al., 2001). Some factors include even more rapid processes, such as earthquakes (Elsworth and Voight, 1995; Elsworth and Day, 1999; Clouard et al., 2001), caldera formation seismicity associated with onshore volcanic edifices (Martí et al., 1997; Hürlimann et al., 2000), and large explosive eruptions (Dávila et al., 2011).

Other factors act over relatively long time periods and are thus considered as preparatory conditions that favour the development of megalandslides. These include stress associated with the extensional regime caused by the main island rift zones (Yepes et al., 2013a) and unloading due to abrasion and onshore erosion which occurs during intensive stages of erosion associated with flank collapse or large rockslides (Yepes et al., 2013b). Deep erosive canyons on the island of Tenerife were identified as playing an important role in the development of landslides (Hürlimann et al., 2004), and intensive erosion is an important element of alternating volcanic build-up and failure cycles (Masson et al., 2002). The occurrence of landslides is probably also affected by site-specific conditions favouring their initiation. These include lithological and structural weakened zones (i.e. ignimbrites,

hyaloclastites, or poorly cemented pyroclasts, vents and volcanic fissures) that control a pressurization response to intrusive events (Elsworth and Voight, 1995; Hürlimann et al., 2001; Rodríguez-Losada et al., 2009). Other factors may also cause large landslides, e.g. stress changes induced by inflation/deflation of magma chambers and hydrothermal reservoirs (Duffield et al., 1982; Lo Giudice and Rasa, 1992; Gudmundsson, 2012), although they have not yet been reported for El Hierro. In some cases, factors that are not directly related to the development of volcanic islands could be a landslide trigger, such as changes in sea level (Carracedo et al., 1999; Ablay and Hürlimann, 2000) or prolonged precipitation (Masson et al., 2002).

In previous research, surprisingly little attention has been paid to the role of inherited rock discontinuities in the development of landslides on volcanic islands (e.g. columnar joints, bedding planes, faults or dykes). This contrasts with DSGSD research, in which numerous studies have demonstrated the significance of fractures resulting from rock formation and later stress forces (Di Luzio et al., 2004; Vilímek et al., 2007; Brideau et al., 2009; Imre et al., 2009; Jaboyedoff et al., 2009). In some cases, even micro-fractures are found to play an important role in landslide development (Zorzi et al., 2014). Nevertheless, some preceding works on volcanic islands have also highlighted the importance of structural conditions for landslide development. Carracedo et al. (2009) stressed the importance of a wedge failure mechanism for their initiation, while Rodríguez-Losada et al. (2009) mentioned the importance of structural weakened zones for large flank collapse and the location of debris avalanche source areas (Seta et al., 2011).

3. Geological and geomorphological setting

The Canary Archipelago, located 100 km off the coast of northwest Africa, is a chain of seven volcanic islands that extends for about 500 km (Fig. 1). El Hierro, with an area of ~269 km^2, is the smallest and south-westernmost island of the Canaries. It has an estimated total edifice volume of 5,500 km^3 and rises about 5,500 m from its submarine base at a depth of 4,000 m b.s.l. (Schminke and Sumita, 2010) to attain an elevation of 1,501 m a.s.l. It is the youngest of the Canary Islands, with its oldest rocks dated to 1.12 Ma (Guillou et al., 1996), and the most recent eruption (Las Calmas Sea submarine eruption) occurring in 2011-2012 (Fig. 1). This eruption was preceded and accompanied by continuous seismicity (López et al., 2012). From its onset, more than 22,000 earthquakes were recorded up to February 2015 (www.ign.es), with local magnitudes of up to 5.1 M_L. Several rock falls took place, caused by the highest magnitude seismic swarms (Jorge Yepes, personal communication).

The geology of this shield volcano consists of three main volcanic cycles (Fig. 1) that correspond to successive volcanic edifices (Guillou et al., 1996; IGME, 2010a, 2010b): the Tiñor Edifice (1.12-0.88 Ma); the El Golfo-Las Playas Edifice (545-176 ka), and the Rifts Volcanism (158 ka-present). The volcanism is characterized by effusive magmatic eruptions of basic composition, which arose through fissure eruptions fed by sub-vertical dykes located mainly along three rift zones (Fúster et al., 1993; Carracedo, 1996; Becerril et al., 2013a, b; Becerril, 2015) with a high concentration of volcanic fissures and vents (Becerril et al, 2015). At least five megalandslides have occurred between the rift axes (Fig. 1) generating steep escarpments and large scars which have notably changed the island morphology (Masson, 1996; Urgeles et al., 1996, 1997; Carracedo et al., 1999; 2001; Gee et al., 2001; Longpré et al., 2011; Masson et al., 2002). The occurrence of these landslides is related to dyke intrusion, pore pressure changes linked to intrusion, seismicity or climatically driven sea-level changes (Masson et al., 2002). Lava injections and associated earthquakes seem to be the most probable triggers of these prehistoric landslides.

Few fragile structures have been reported in the western and southern rifts (Becerril, 2014, 2015). However, a clear system of sub-vertical dislocation planes, striking ENE-WSW, has been described only along the north-eastern rift (Day et al., 1997; Carracedo et al., 2001; IGME, 2010a; Becerril et al., 2015) forming the so-called 'San Andrés Fault System'. Its fault scarps and planes form the scarps and slip planes of the SAL. The SAL (Fig. 1) is referred to as Las Playas I in Masson et al. (2002) and the San Andrés slump in Gee et al. (2001). In this article we refer to the San Andrés Landslide (SAL, Fig. 1). The age of the SAL was constrained by Gee et al. (2001) to 176-545 ka. This landslide has been interpreted as an aborted, inactive giant flank collapse (Day et al., 1997) but other authors (Gee et al., 2001) concluded that it is a partly failed slump, where movement occurred in several phases, providing suitable conditions for the occurrence of the younger Las Playas II debris avalanche (145-176 ka; Gee et al., 2001). The accumulation of the Las Playas II debris avalanche is partly superimposed over the SAL deposits, providing evidence of the relative timing of both of the events (Gee et al., 2001).

4. Applied methods

To obtain novel information about the SAL we applied methods widely used in DSGSD research, which have never before been applied in the study area. They include a detailed morphological study of the SAL, an in-depth study of structural conditions at site-specific and regional scales (e.g. valley network analysis), and we also installed direct movement monitoring on the possible future sliding planes of the SAL.

We used a morphological approach to identify and describe the limits and surface forms found within the SAL. Due to the character of the landslide, we focused on diagnostic features of DSGSDs (i.e. scarps, antithetic scarps, double-crest ridges, trenches) and

identification of the secondary landslides. The latter is commonly used to identify most landslide-prone regions as well as actively deforming segments within DSGSD bodies (Crosta et al., 2014).

Structural conditions were documented within secondary landslides as well as fractures along the sliding planes. This information with the slope geometry can be used for the identification of kinematically suitable areas for rockslide development (Günter, 2003; Santangelo et al., 2015) and also to explain the occurrence conditions of DSGSDs (Pánek et al., 2011). We applied this approach to test structural influences on the development of the SAL and the secondary landslides that occur on its body. Possible prevailing effects of structural conditions on long-term relief development at a regional scale were tested by an analysis of the valley network. This analysis provides information on the long-term surface development controlled by lithological, structural and morphological characteristics, regardless of actual surface hydrology (Horton, 1945; Křížek and Kusák, 2014). We were looking for evidence of specific structural conditions occurring within the SAL, both showing its unique properties compared to the rest of the island and complementing our site-specific structural study. We decided not to use lineament mapping for this purpose as the results would partly overlap with the valley network analysis and the already available structural and volcano-structural mapping (Becerril, 2014).

Finally, we installed three very precise (10^{-2} mm), 3D optical-mechanical crack gauges (Košťák, 2006; Klimeš et al., 2012) to measure movements along discontinuities assumed on the basis of field mapping to represent slip planes of the SAL. The high frequency deformation readings provide accurate and representative information about the recent activity of the SAL.

4.1. **Geomorphological mapping**

Five topographic profiles were constructed and then analysed for the presence of typical DSGSD morphological features (e.g. scarps, antithetic scarps, inclined planes, trenches). The profiles were constructed using a Digital Elevation Model (DEM) provided by the National Geographic Institute (IGN; http://centrodedescargas.cnig.es/) with 5 m cell dimensions. The DEM was generated in 2009 using cubic convolution interpolation of LiDAR point-clouds (density 0.5 point/m^2, precision 0.5-1 m RMSZ) acquired by IGN/PNOA (2015). We also used bathymetric data to make a DEM for the submarine part of the SAL. The bathymetric data show contour lines with 100 m intervals (GRAFCAN, 2009) depicting only general morphology of the submerged part of the landslide.

Through fieldwork, DEM analysis and interpretation of colour aerial photographs (pixel size of 0.25 m) we mapped the aforementioned DSGSD indicative landforms, including secondary landslides, at a scale of 1:5,000. Landslides were mapped only if it was possible to clearly identify their scarp area, landslide body, or landslide accumulation. Less preserved landslide forms were omitted, as were landslides whose one dimension did not exceed 80 m. The mapped landslides included rockslides, landslides in colluvium, and deep-seated block slides. The deep-seated block slides are represented by headscarps detaching largely undisturbed blocks of rocks which often have a plane surface with a slight counter slope inclination. Other landslide types follow the definitions given in Cruden and Varnes (1996).

4.2. **Structural measurements and kinematics**

During the field mapping we collected 253 structural measurements characterizing dip and dip direction of SAL scarps and antithetic scarps. Slickensides of the SAL scarps were also measured in fourteen cases and its kinematics were analysed in GEOrient©. Fractures and

bedding planes were measured mainly within the mapped shallow landslides and inside the Tijirote water gallery (Fig. 1). We also focused on collecting different sets of pre-existing discontinuities (i.e. fractures, bedding planes), which could act, based on the field observations, as detachment planes for landslides. Their geometric alignment (dip, dip direction), with slope geometry (slope dip and aspect), was tested using the topography bedding-plane intersection angle (TOBIA index), according to Meentemeyer and Moody ((2000) and for rock slope stability assessment (Günter 2003). The latter method determines areas where sliding is possible based on the attitude of the assumed slip planes (e.g. structural elements) and the slope surface with gravitational force being the destabilizing factor, which is balanced by the internal friction angle of the rock slip planes. Different sets of bedding planes and fractures, including SAL slip planes and the hypothetical basal sliding plane suggested in Elsworth and Voight (1995), were tested as potential planes of weakness. The analysis tests only geometric constraints of landslide development without any lithostatic pressure. We used the IDW interpolation algorithm to calculate Digital Structural Models (DSM) of the selected structural elements measured in the field. The DSM for the SAL slip planes was based on spatially distributed field data, whereas the DSM of fractures and bedding planes represented single dip direction and dip values which were determined to be the most frequently present at the studied sites (cf. the method used in Pánek et al., 2011). The internal friction angle values used in testing of landslide occurrence were applied over a range between 20° and 60° as used in the calculations of Elsworth and Voight (1995). A lower threshold of 10° was also tested. Such low values of internal friction angles were suggested by Rodríguez-Losada et al. (2009) for poorly cemented pyroclastic rocks on slopes higher than 1,500 m, which correspond with the potential sliding planes located on the submarine part of the island. Similar low values of internal friction angles were determined for a residual friction angle of thin clay layers within DSGSDs in the flysch rocks (Fekeč et al. 1970),

which we assume could be analogous to the material found as a thin clay layer on the SAL slip plane inside the Tijirote water gallery (Fig. 1, 2). This material was tested to determine its basic mechanical properties, allowing an estimation of the internal friction angle. Granulometry, Atterberg limits and unit weight were determined according to AENOR (1993, 1994a, 1994b, 1994c) and the material was classified using the United Soil Classification System (USCS, ASTM 2006). Mineralogy, with special attention to clay minerals was examined by X-ray diffraction analysis and processed using XPowder® software (Martín-Ramos, 2004), based on a reference database of diffractograms and following the process designed by Snyder and Bish (1989) and Downs and Hall-Wallace (2003).

The methodological constraints of the kinematic testing implies that the results represent theoretical scenarios defined by measured or assumed structural conditions, actual slope geometry and suggested properties of possible sliding planes, rather than a stability assessment of the studied slopes.

4.3. **Valley network analysis**

Morphometric characteristics of the valley network for the entire island of El Hierro were calculated. These characteristics indicate structural development and morphological and lithological characteristics of specific areas (Horton, 1945; Křížek and Kusák, 2014). The valley network was derived from the available DEM using the HydroTool script in 10.2 ArcGIS (ESRI©) software. A flow accumulation raster was aggregated and classified as a valley when the value of flow accumulation was >25 m^2. Each valley was assigned an order using the Gravelius order system that defines the order of the valley network in the direction from the outfall towards the valley head (Gravelius, 1914, in Zăvoianu et al., 2009).

According to Křížek and Kusák (2014), the following morphometric characteristics (sensu Horton, 1945) are the most suitable for valley network identification:

a) 'Valley junction angles' express the angle at which the subsidiary valley runs into the main valley projected on a horizontal plane;

b) 'Number of valleys' *n* was determined as the number of all valleys of the given order (sensu Zăvoianu et al. 2009) in the valley network;

c) 'Total lengths of valleys' *t* was defined as the sum of the lengths of all valleys of the given order in the valley network;

d) 'Valley network density' *D* was defined by the equation: $D = L / P$, where L is the total length of thalwegs and *P* is the area of El Hierro.

4.4. **SAL monitoring**

Direct point measurements of DSGSD movement activity are considered to be a reliable source of information on their recent development dynamics (Booth et al., 2015). Several DSGSD cases in a variety of geological conditions have been monitored for protracted time periods using a TM-71 crack gauge (Košťák, 2006; Klimeš et al., 2012). Information about the limits and morphology of a landslide are necessary for selection of proper monitoring sites. Field inspection of these features identified the future installation sites, bearing in mind all of the technical requirements described in detail in Klimeš et al. (2012). Three instruments were installed on the SAL to monitor possible movements on discontinuities which represent the main or suggested SAL scarps or slip planes (Fig. 1).

Crack gauge HIE1 monitors a suggested slip plane (previously described as a fault plane in Becerril, 2014) located about 900 m inside the Tijirote water gallery, at an elevation of 484 m a.s.l. (Fig. 1, 2). This slip plane is not manifested by a scarp in the relief. Thus, it is

difficult to judge if the apparent evidence of movement along this plane developed due to tectonic forces or as a result of gravitational deformation. The slip plane dip and dip direction are 60°/114°. It has developed in fractured olivine-pyroxene massive basalts and the fracture is filled with soft clays with preserved slickensides (Fig. 2).

Crack gauge HIE2 measures movements on the most prominent relief manifestation of the SAL slip plane (75°/140°) described by previous works as a fault plane (Fig. 2; Day et al., 1997; Carracedo et al., 2001). One arm of the instrument is drilled into olivine-pyroxene massive basalts, while the opposite arm is fixed into a large concrete cube with dimensions of 1 ×1 ×1 m, placed into the talus deposits below the rock face with a preserved fault plane.

The third instrument, HIE3, is fixed into scoriaceous basalts dissected by the SAL scarp up to 1.8 m in height, and trending E-W (89°/189°) with occasionally preserved slickensides, suggesting sinistral movement dipping 40° towards the east (Fig. 3). The geotechnical properties of this kind of rock can be found in Rodríguez-Losada et al. (2007). All three crack gauges are equipped with automated data recorders allowing collection of measurements with high temporal frequency, and their semi-automated processing considering the actual air temperature (Marti et al., 2013). The current reading interval is set at a frequency of 24 hours, which is more regular than in other previous studies (Klimeš et al. 2012), where slow-moving DSGSDs were monitored using a TM-71 crack gauge usually once a month.

Stresses associated with seismic events are thought to play an important role in the triggering of deep-seated landslides on volcanic islands (Gee et al., 2001). Therefore we combined the landslide movement measurements with the available earthquake database created by IGN and publically available on its website (www.ign.es/ign/resources/volcanologia/hierro.html).

5. **Research results**

5.1. **Geomorphological mapping**

5.1.1. SAL morphology

On-shore limits of the SAL, to the north and northwest, are morphologically well-defined (Fig. 3, profiles A-A´ and B-B´ on Fig. 4), as previously described Day et al. (1997). On the other hand, the western and southern borders of the SAL do not follow clearly pronounced morphologic features (Fig. 3) and are a hypothetical limit defined on the basis of the local geomorphology, including a gully (No. 1 in Fig. 3) interpreted as a remnant of a side scarp. The SAL limits defined in this way differ from those described by Day et al. (1997) and do not resemble the typical horseshoe shape of other scarps in El Hierro, such as El Golfo or El Julan landslides (Fig. 1).

A wide and shallow trench below the main scarp of the SAL (No. 2 in Fig. 3, profile B-B´ in Fig. 4) is formed by antithetic scarps while other trenches associated with antithetic scarps are deeper and narrower. Younger volcanic rocks bury earlier scarps, smoothing the slope morphology, as illustrated by the 'profile overlay' inset in Fig. 4. Profiles with exposed older rocks (profiles A-A´ and C-C´ at elevations of between 650 and 200 m a.s.l.) have clearly visible scarps and antithetic scarps, while these features are less visible on areas covered by younger lavas, with a general slope of about 19°.

The parallel profile towards the coast (E-E´) shows the asymmetry of the slopes to the southwest and northeast of the SAL. The former fall abruptly into the main Las Playas scarp while the latter are gentler slopes. The whole E-E´ profile exhibits a general drop in elevation towards the northeast which is better visible within the SAL. This profile, along with the

DEM, shows that the area of the SAL is segmented by distinct morphological features running roughly perpendicular at each other and dissecting the area into large blocks, generally dipping towards the northeast. These blocks are separated by northwest-southeast oriented gullies. The heads of the gullies are located close to the ridge and expose rocks from the older volcanic edifices.

5.1.2. Offshore morphology of the SAL

The northern shoreline of the SAL forms a wide bay where the port of Estaca is located (No. 3 in Fig. 3). This bay is associated with the older Tiñor volcanic sequences (Fig. 1) and hosts the three best-developed gullies within the SAL, as well as across the whole island. Furthermore, the study of Masson et al. (2002) shows notable differences between the offshore morphology and the composition of the deposits of the El Golfo and El Julan megalandslides, with respect to those of the SAL. The first two morphologies show evidence of underground flows and accumulations, whereas the SAL offshore area does not show any clear evidence of similar processes and exhibits a wide number of ridges and blocks unlike the two others landslides. Some of these are associated with eruptive fissures and volcanic vents identified by Becerril et al. (2015). These vents exhibit a different pattern compared to the other parts of the submarine slopes, where they spread out radially offshore. In the case of the SAL, these features have arched forms resembling the main onshore structural forms of the landslide.

5.1.3. Secondary landslides on the SAL

Fig. 3 shows the uneven distribution of the mapped features, mainly of the shallow debris flows and rockslides, which are found in the northern part of the SAL. The rockslides are limited to the pyroclastic rocks that preceed the maximum glacial period. Their head scarps and sliding planes are controlled by structural and lithological properties of the rocks with bedding planes dipping towards the south or southeast with an inclination of about 30°. Head scarps are usually bounded with steeply inclined (65°-85°) fractures dipping towards the SSE (155°) and WSW (260°). Colluvial landslides (e.g. No. 4 in Fig. 3) occur near the main landslide scarp or the antithetic scarps, mobilizing highly fractured and weathered rocks. In contrast, the distribution of deep-seated block slides is limited to well-developed gullies in the central part of the SAL (Fig. 3). They are detached along scarps ranging from 2 m to 100 m (No. 5 in Fig. 3), suggesting considerable depths of their slip surfaces. Plane surfaces developed below the scarps dipping slightly against the slope possibly suggest rotation and back tilting of the slid blocks. Nevertheless, bedding of the rock sequence clearly visible on the gully slopes does not confirm this assumption. Remnants of the deep-seated block slides (No. 6 in Fig. 3) buried by younger lava flows have a back-tilted plane surface placed exactly at the same altitude, as in the case of the deep-seated block slide No. 3 (Fig. 3).

5.2. **Structural setting of the SAL**

The inset in Fig. 3 also provides an overview of the structural conditions found within the SAL, showing two prevailing crack families both mainly dipping steeply. One group of crack measurements is generally dipping towards the southeast and includes only measurements from scarps of the SAL (a in Fig. 3), some of which do not have any associated morphological evidence (e.g. the suggested slip plane monitored by HIE1 inside the Tijirote water gallery). The second family dips generally in the opposite direction, towards the

northwest, and represents antithetic scarps (a in Fig. 3), with a lower dip (below 40°). A similar pattern was found within the measurements of fractures (b in Fig. 3). Unlike the scarp measurements, the minor crack families are steeply dipping toward the northeast and west-southwest, which are not present among the fault measurements. Bedding planes (c in Fig. 3) dip uniformly towards the southeast, with a prevailing inclination of about 30°.

The structural properties of the selected landforms were investigated in detail. Rock slides developed within pyroclastic rocks are determined by shallow-dipping bedding planes and a set of cracks (Fig. 3) that follow the general SAL scarp direction, dipping towards the southeast, or include steeply northeast- and west-dipping cracks (e.g. rock slide No. 1 in Fig. 3). Structural measurements within the deep-seated block slide revealed discontinuities along where the slide detached and which correspond to the SAL scarp direction. Shallow-dipping cracks (block landslide in Fig. 3) with two different dip directions represent a displaced and disturbed rock mass within the block slide. The structural setting description was also confirmed by measurements along the 900 m-long Tijirote gallery. Discontinuities corresponding to the SAL scarp were detected along two other groups of cracks. One can be attributed to the antithetic scarp family while the other to the transversal cracks dipping to the northeast.

5.3. **Kinematic testing of landslide occurrence conditions**

Planar failure mechanism constrained by surface morphology (DEM) and spatially distributed structural measurements of the SAL scarps and related discontinuities (DSM) is a feasible only for very limited areas. They are largely contained within the three deep-seated block landslides identified during the field mapping (No. 1 in Fig. 5). The spatial distribution of the susceptible areas remains almost unchanged within the interval of 10°-25° of the applied

internal friction angle. When its value is increased to 40°, the susceptible area is reduced within the large deep-seated block failure (No. 4 in Fig. 3) with suitable conditions for the development of instability.

Kinematic testing of planar failure constrained by the subaerial and submarine morphology of the SAL, and a theoretical basal sliding plane (dip of 6° taken from Elsworth and Voight, 1995) with assumed dip directions in the range of 135°-155°, did not show any susceptibility to landsliding when the angle of internal friction was set within the suggested value range of 10°-60°. Only when the angle of internal friction was reduced to less than 7° did a large part of the onshore as well as offshore study area become susceptible to this failure mechanism (No. 2 in Fig. 5). Similar results were obtained when testing the wedge failure mechanism defined by a hypothetical basal sliding plane and the DSM characterizing the SAL scarps. This failure mechanism is feasible for the majority of the study area only when reducing the angle of internal friction to an unrealistic value of 3° (No. 2 in Fig. 5).

Analysis of the infill material of the potential SAL slide plane inside the Tijirote gallery provides only limited insight into the possible strength properties affecting landslide stability. It showed that the most abundant minerals of the fine-grained material mainly composed of silty sand with low clay content (Table 1) are clinopyroxene, plagioclase with minor constituents of feldespathoids, oxides, and phyllosilicates. The most abundant clay mineral is the highly expandable smectite, which has unfavourable properties for slope stability. Unfortunately, the high content of fine-grained material and the presence of smectite makes it impossible to reasonably estimate the internal friction angle (cf. Novotný and Klimeš, 2014), which could be used to better specify the possible sliding conditions in the kinematic analysis.

5.4. **Valley network analysis**

Some 3,280 valley channels, grouped into five orders, were identified on El Hierro. Based on the morphology of the island and the identified drainage basins, we divided the island into regions for which the characteristics of the valley network were calculated separately (Fig. 6). Some of the four regions near the SAL have unique characteristics compared to the rest of the island (Table 2). The valley junction angles reached values 32% higher within the northern part of the SAL than any other parts of the island (SA North in Table 2). The valley network of SA South and Punto Limpio (Fig. 5) as well as for the rest of the island is parallel, with streams following the highest slopes - as commonly occurs in structurally undisturbed volcanic edifices (Becerril, 2014). In contrast, the Tiñor edifice shows dendritic and SA North rectangular valley networks, with the most frequent valley junction angles being between 80 and 90° (76°21´ in Table 2). Dendritic valley networks are generally present in regions with homogenous geology and uniform relief inclination with very limited structural influences (Howard, 1967; Price, 1986; Husain, 2008). On the other hand, the rectangular valley network is evidence for the presence of structurally-induced linear features (e.g. concealed faults, fractures and joints), which are being followed by the streams (Howard, 1967; Gabler et al., 2008) and often run roughly perpendicular to the highest slope direction. Furthermore, the valley network densities in the Tiñor edifice and SA North are extremely low, comparable only to the Las Playas valley basin with a value of 0.0056 m m^{-2}. Low valley network densities are attributed to regions with increased water infiltration compared with surface runoff (Pradhan et al., 2009). This may possibly increase the amount of water in the bedrock, which creates more suitable conditions for landslide initiation due to the increased water pressure during magma injections.

5.5. **Monitored movements**

The movements measured by the TM-71 crack gauges between February 2013 and August 2014 are summarized in Fig. 7. Measurements from the HIE1 gauge show no movement during the entire monitoring period. In contrast, measurements from the HIE2 gauge show a total of 0.22 mm of progressive sinistral strike slip (y-axis) for the whole of the monitoring period. The x-axis predominately shows extensional movement, which changed to compression for a few months at the beginning of 2014. The z-axis (vertical component) shows general stability throughout the monitoring period.

Measurements from the HIE3 gauge were taken manually for most of 2013, with an automated data acquisition system installed at the end of November 2013. These measurements show long-term sinistral strike slip movements of 1.1 mm, which ceased in April 2014. The x-axis shows slow extensional movement with a strong compression pulse of 0.65 mm during December 2013. The z-axis shows slight movement of the downslope block in the upslope direction for most of the monitoring period.

6. **Discussion**

6.1. **Recent activity and future development of the SAL**

No previous literature dealing with the SAL explains in detail why the originally fast-moving landslide (Carracedo, 2008) stopped and afterwards stood still. One hypothesis suggests that the landslide stopped due to the lack of pressurized water in the fault system resulting in an ‘aborted’ landslide (Day et al., 1997). This theory explains the termination of one fast moving episode but does not explain why the already in progress, and thus weakened, landslide mass did not reactivate or could not reactivate into a major movement in the geological future. To

answer this question we summarized the new findings on results of the direct monitoring of the main SAL scarps and evidence from previous work:

a) The unique morphological manifestation of the main scarp of the SAL (which is often referred to as the San Andrés Fault) may reflect its unique formation conditions controlled by landslides under creep movement activity.
b) Structural research showed that several discontinuity sets favouring landslide occurrence are present within the SAL.
c) Fragmentation of the rock mass revealed by field measurements at specific sites is reflected by landforms on a slope scale (e.g. scarps, antithetic scarps, trenches, gullies) and a valley network pattern which has unique properties compared to the rest of the island.
d) There is evidence of weakened zones that possibly facilitate shear plane development represented by eruptive vents (Carracedo et al., 1998) or eruptive vents and fissures (Becerril et al., 2013a) located to the north and west, just outside the limit of the landslide.
e) Over one year of direct surface monitoring, creeping on the main SAL sliding planes is shown.
f) Creep movement within the SAL is also demonstrated by the clay infill of the potential slip plane inside the Tijirote water gallery, which may be interpreted as a retrogressive landslide slip plane.
g) The morphology of the SAL offshore region is evidence of its young development stage (less mature), compared to other landslides on El Hierro. We also argue that the environmental and geological conditions remain favourable for possible future activity of the SAL.

h) The landslide maintains high onshore relative relief (1000 m over a distance of 3.5 km) while the GPS monitoring operated by the IGN determined growth of the island (www.ign.es; López et al., 2012).

i) No permanent support of its toe was identified onshore, while offshore accumulation is partly covered by the later Las Playas debris avalanche which may provide some support to the distal part of the SAL accumulation.

j) Marine abrasion and river incision act especially on its north-eastern part causing permanent unloading of the toe of the landslide.

k) Possible triggers of accelerated landslide activity occur on the island, i.e. earthquakes, magma intrusions, opening of volcanic vents. However, others cannot be excluded (e.g. extreme precipitation).

In addition to the aforementioned indirect evidence for conditions favouring continuous landslide development, we may use an analogy with DSGSDs where spatial and temporal movement patterns are better described. Many authors indicate that creep could accelerate into sliding (e.g. Terzaghi, 1950; Moon and Simpson, 2002; Baldi et al., 2008) and also show that repeating activity of DSGSDs or their parts is common in a variety of environments (Moro et al., 2007; Vilímek et al., 2007; Klimeš et al., 2009a; Klimeš et al., 2009b; Pánek et al., 2011; Crosta et al., 2004; 2014). This also includes volcanic islands where continuous creep or repeating sliding activity of similar landslides has been described in other works (Pararas-Carayannis, 2002; Seta et al., 2011; Hunt et al., 2011). All of the above-mentioned findings suggest continuing development of the SAL in the future.

It is difficult to determine the magnitude of possible future movements, which may be represented by velocities varying from creep to sliding, affecting the entire SAL or its parts. Also, the possible absolute magnitudes of horizontal or vertical movements along the main sliding planes are very difficult to estimate. The limited historical information about

reactivations of similar deep-seated landslides on volcanic islands (Carvelli et al., 2000) shows that movements reaching only up to tens of meters may occur during a single sliding phase. This uncertainty about future landslide development hinders reliable assessment of potentially catastrophic effects induced by the landslide reactivations which may also generate tsunamis.

There is a possibility that the SAL may undergo an accelerated movement phase affecting only part of its entire area. This suggestion is supported by a closer look at the SAL morphology and the possibility that the Las Playas I debris avalanche could represent a partial reactivation of the region, which previously formed part of the SAL. Partial reactivation of the SAL is further supported by our geomorphological research which identified two main parts of the SAL divided by a morphological line in the northwest-southeast direction (Balón ravine, No. 7 in Fig. 3). In general, the north-eastern part has more secondary landslides, scarps and antithetic scarps (Fig. 3); it is more dissected by streams which form deep gullies; there are abundant volcanic cones along or close to its limits; on-shore there are much steeper and higher slopes forming cliffs; and it is built in older rocks from the Tiñor eruptive phase. On the other hand, younger rocks cover the south-western part; there are less landslides and much less morphologically evident scarps and antithetic scarps; the morphology is mostly uniform with less developed gullies; and the shore is shallow and flat without cliffs. This suggests higher susceptibility to increased landslide activity for the north-eastern part of the SAL. The same conclusion can be drawn when evaluating diagnostic features suggested by Hürlimann et al. (2004). The north-eastern part of the SAL contains two of four such features (presence of deep erosive gullies and coastal cliffs) while none are present in the south-western part.

In addition to the morphological features, a high susceptibility to the opening of new eruptive vents was calculated for the area close to the north-eastern part of the SAL (Becerril

et al., 2013a). Such a process may cause an increase in fluid pressure and stress, which could be capable of triggering the sliding movement along pre-existing weakened plains (e.g. the possible SAL scarp inside the Tijirote gallery). Nevertheless, there is still an unanswered question about the intensity of the potential triggering events required to cause significant movement of the SAL. For example, the Las Calmas Sea submarine eruption event, accompanied by thousands of earthquakes with a magnitude of up to 5.1 M_L, did not reactivate the SAL scarps nor did it cause any remarkable secondary landslides. It is also suggested that the occurrence of the younger El Golfo landslide did not trigger major activity of the SAL (Carracedo et al., 1999) despite its close proximity to the SAL scarp area.

6.2. **Suggested areas for future research**

Despite a variety of evidence suggesting that the structural conditions play an important role in the initiation and development of the SAL, the performed kinematic testing did not provided a clear answer to its role in the overall slope stability of the landslide. However, it did prove that a planar failure mechanism is realistic for secondary deep-seated block landslides. The validity of this finding for the entire SAL is difficult to judge because of the simplicity of the applied slope stability approach. Namely, the estimated values of angle of internal friction are the only parameters describing the strength of the material that is possibly subject to the sliding. Moreover, the SAL sliding plane located at an unspecified depth has unknown and probably complex shape and there is an uncertainty in describing the structural settings in these depths using superficial measurements. The latter seems to be a reasonable approximation of the in-depth structural conditions, as shown by structures parallel to the rift (e.g. dykes, volcanic fissures) which cross-cut the entire subaerial part of the island (Carracedo et al., 2001). Assumptions about depth uniformity could only be applied to all of

the tested structural surfaces, planar or wedge failures, if unrealistically low (3°-7° of the angle of internal friction) strength parameters on the failure planes are considered. The properties of the infill material acquired from the potential sliding plane in the Tijirote gallery do not suggest such a low strength. Nevertheless, the presence of expandable clays in the stuffed joints and their fine-grained composition, make favourable conditions for a significant reduction in strength when additional destabilizing forces may act (e.g. pressurized water, ground acceleration during earthquakes). Therefore, a better understanding of the geometry of the basal sliding plane and the relevant rock strength parameters is necessary for the reliable quantification of the slope stability of large landslides on volcanic islands. To achieve this, numerical modelling and rock strength testing under representative conditions (Sassa et al., 2014) would be necessary. Also, analogue models of the landslides may be useful for understanding their internal structure and possible movement mechanisms (Bozzano et al. 2013).

Another field of study which requires continuous attention is monitoring of the landslide movements. The first approach was considered by establishing the monitoring network using TM-71 gauges. The initial results proved the correct selection of the monitoring sites: none of them exhibit simple downslope gravitational movement which would mean that the monitoring is biased by rather shallow slope deformations affecting the surface measurements. The results also largely correspond to our assumptions based on the field observations, which suggested higher movement activity on sites HIE2 and HIE3 compared to site HIE1, which is located on a plane with no clear morphological manifestation on the surface and outside the previously identified landslide limits (e.g. Day et al., 1997). The instrument at this location has not yet shown any movement, whereas the two other instruments detected sinistral movements. This movement pattern is in accordance with its suggested kinematics interpreted based on the morphological and slickenside analysis (Fig.

3). Nevertheless, one year of deformation monitoring along the sliding plane and scarps of the landslide is a very short period of time to make any strong conclusions, especially regarding long-term deformation behaviour. Only protracted monitoring would be able to clarify whether the detected creep is a response to the increased seismic activity following the Las Calmas Sea submarine eruption (2011-2012), or it represents long-term movement activity of the SAL. We suggest that the only reliable way for hazard assessment is simultaneous monitoring of the landslide movements and related geodynamical processes (e.g. earthquakes, surface movements, volcanic activity), which may eventually detect and explain movement accelerations and their possible causes.

7. Conclusions

Morphological and structural data of the San Andrés Landslide show unique properties on the island of El Hierro. The landslide is limited by very well preserved and pronounced scarps (no similar features have been identified on any of the other Canary Islands); the valley network within the SAL shows a different pattern to the rest of the island, being dissected with deep gullies not found outside the landslide area; and regarding its offshore body, it shows unique characteristics compared to other landslides on the island, as it has been previously suggested by other research. The evidence suggests that the north-eastern part of the landslide is more susceptible to future reactivations. In addition, the environmental and geological conditions affecting slope stability within the entire landslide (e.g. sea abrasion, repeating volcanic events and earthquakes, volcanic growth) favour future landslide development over its long-term stability. The one-year direct monitoring of movements on three selected slip planes showed predominantly sinistral strike slip movement of up to 1.1 mm, proving the creep activity of the landslide. However, the monitoring period coincided with a seismo-volcanic

unrest that could have reactivated the sliding planes. This direct and indirect evidence suggests on-going development of the San Andrés Landslide, illustrating its role in the recent as well as future evolution of the youngest island of the Canary Archipelago. Nonetheless, a reliable description of the magnitude, temporal and spatial patterns of the future landslide development still requires further investigation, during which a long-term monitoring is the only reliable and applicable approach to a more precise sliding hazard assessment. The presented work shows that a detailed site investigation is required to acquire relevant information for hazard assessment (including the possibility of tsunami wave generation) of any large landslide on a volcanic island, especially on fast growing and high populated islands such as the Canaries.

Acknowledgements

The authors would like to thank the National Geographic Society/Waitt Grants Program (No. W244-12) and CzechGeo/EPOS (Project No. LM2010008) for the financial support of the research. We also thank the Spanish National Geographical Institute and the El Hierro Island Authority whose personnel provided us with useful support during the field installation of the measuring instruments. This work was carried out thanks to the unconditional support of the long-term conceptual development research organisation RVO: 67985891.

References

Ablay, G., Hürlimann, M., 2000. Evolution of the north flank of Tenerife by recurrent giant landslides. Journal of Volcanology and Geothermal Research, 103, 135-159.

Acosta, J., Uchupi, E., Muñoz, A., Herranz, P., Palomo, C., Ballesteros, M. and ZEE Working Group, 2003. Geologic evolution of the Canarian Islands of Lanzarote, Fuerteventura, Gran Canaria and La Gomera and comparison of landslides at these

islands with those at Tenerife, La Palma and El Hierro. Marine Geophysical Researches, 24, 1-40.

AENOR, 1993. UNE 103-104/93 Test for the plastic limit of a soil. Asociación Española de Normalización y Certificación, Madrid, Spain.

AENOR, 1994a. UNE 103-301/94 Determination of a soil density, Method of the hydrostatic balance. Asociación Española de Normalización y Certificación, Madrid, Spain.

AENOR, 1994b. UNE 103-302/94 Determination of the relative density of the particles of a soil. Asociación Española de Normalización y Certificación, Madrid, Spain.

AENOR, 1994c. UNE 103-103/94. Determination of the liquid limit of a soil by the Casagrande method. Asociación Española de Normalización y Certificación, Madrid, Spain.

Agliardi, F., Crosta, G., Zanchi, A., 2001. Structural constraints on deep-seated slope deformation kinematics. Engineering Geology 59 , 83-102.

ASTM International, 2006. Designation D 2487-06 Standard Practice for Classification of Soils for Engineering Purposes (Unified Soil Classification System).

Baldi, P., Cenn,i N., Fabris, M., Zanutta, A., 2008. Kinematics of landslide derived from archival photogrammetry and GPS data. Geomorphology 102, 435-444.

Becerril, L., 2014. Volcano-structural study and long-term volcanic hazard assessment on El Hierro Island (Canary Islands). Ph.D. Thesis. University of Zaragoza, Spain. ISBN: 978-84-617-3444-3.

Becerril, L., Cappello, A., Galindo, I., Neri, M., Del Negro, C., 2013a. Spatial probability distribution of future volcanic eruptions at El Hierro Island (Canary Islands, Spain). Journal of Volcanology and Geothermal Research, 257, 21-30.

Becerril, L., Galindo, I., Gudmundsson, A., Morales, J.M., 2013b. Depth of origin of magma in eruptions. Scientific Reports, 3, 6.

Becerril, L., Galindo, I., Martí, J., Gudmundsson, A., 2015. Three-armed rifts or masked radial pattern of eruptive fissures? The intriguing case of El Hierro volcano (Canary Islands). Tectonophysics, doi: 10.1016/j.tecto.2015.02.006.

Booth, A. M., Dehls, J., Eiken, T., Fischer, L., Hermanns, R. L., Oppikofer, T., 2015. Integrating diverse geologic and geodetic observations to determine failure mechanisms and deformation rates across a large bedrock landslide complex: the Osmundneset landslide, Sogn og Fjordane, Norway. Landslides, 12, 745-756.

Bozzano, F., Bretschneider, A., Esposito, C., Martino, S., Prestininzi, A., Scarascia Mugnozza, G., 2013. Lateral spreading processes in mountain ranges: Insights from an analogue modelling experiment. Tectonophysics, 605, 88-95.

Brideau, M. A., Yan. M., Stead, D., 2009. The role of tectonic damage and brittle rock fracture in the development of large rock slope failures. Geomorphology 103, 30-49.

Carracedo, J.C., 1996. Morphological and structural evolution of the western Canary Islands: hotspot induced three armed rifts or regional tectonics trends? Journal of Volcanology and Geothermal Research, 72, 151-162.

Carracedo, J.C., 2008. Canarian volcanoes, IV. La Palma, La Gomera, El Hierro. Editorial Rueda S.L., Madrid.

Carracedo, J.C., 2014. Structural Collapses in the Canary Islands. In: Gutiérrez, F., Gutiérrez, M. (Eds.), Landscapes and Landforms of Spain. Springer, pp. 289-306.

Carracedo, J.C., Day, S., Guillou, H., Rodríguez Badiola, E., Canas, J.A., Pérez-Torrado, F.J., 1998. Hotspot volcanism close to a passive continental margin: the Canary Islands. Geological Magazine, 135, 591-604.

Carracedo, J.C., Day, S.J., Guillou, H., Torrado, F.J.P., 1999. Giant Quaternary landslides in the evolution of La Palma and El Hierro, Canary Islands. Journal of Volcanology and Geothermal Research, 94, 169-190.

Carracedo, J.C., Rodríguez Badiola, E., Guillou, H., de La Nuez, H.J., Pérez Torrado, F.J., 2001. Geology and volcanology of the Western Canaries: La Palma and El Hierro. Estudios Geológicos, 57, 171-295.

Carracedo, J.C., Pérez Torrado, F.J., Paris, R., Rodríguez Badiola, E., 2009. Megadeslizamientos en las Islas Canarias. Enseñanza de las Ciencias de la Tierra, 17, 44-56.

Cervelli, P., Segall, P., Johnson, K., Lisowski, M., Miklius, A., 2000. Sudden aseismic fault slip on the South Flank of Kilauea volcano. Nature, 415, 1014-1018, doi:10.1038/4151014a.

Cimarelli, C., de Rita, D., 2010. Deep-seated gravitational slope deformations in volcanic settings: examples from Italian volcanoes. Geografia Fisica e Dinammica Quaternaria, 33, 155-164.

Clouard, V., Bonneville, A., Gillot, P.Y., 2001. A giant landslide on the southern flank of Tahiti Island, French Polynesia. Geophysical Research Letters, 28, 2253-2256.

Crosta, G.B., Chen, H., Lee, C.F., 2004. Replay of the 1987 Val Pola landslide, Italian Alps. Geomorphology, 60, 127-146.

Crosta, G.B, di Prisco, C., Frattini, P., Frigerio, G., Castellanza, R., Agliardi, F. (2014): Chasing a complete understanding of the triggering mechanisms of a large rapidly evolving rockslide. Landslides, 5, 747-764, doi: 10.1007/s10346-013-0433-1

Cruden, D. M., Varnes, D. J., 1996. Landslide types and processes. In: Turner, A. K., Shuster, R.L. (Eds.), Landslides: investigation and mitigation. Transportation Research Board, Special Report 247, pp 36-75.

Dávila, P., Branney, M.J., Storey, M., 2011. Large eruption-triggered ocean-island landslide at Tenerife: Onshore record and long-term effects on hazardous pyroclastic dispersal. Geology, 39, 951-954.

Day, S.J., Carracedo, J.C., Guillou, H., 1997. Age and geometry of an aborted rift flank collapse: the San Andres fault system, El Hierro, Canary Islands. Geological Magazine, 134, 523-537.

Di Luzio, E., Saroli, M., Esposito, C., Bianchi-Fasani, G., Cavinato, G. P., Scarascia-Mugnozza, G., 2004. Influence of structural framework on mountain slope deformation in the Maiella anticline (Central Apennines, Italy). Geomorphology 60, 417-432.

Downs, R.T., Hall-Wallace, M., 2003. The American mineralogist crystal structure database. American Mineralogist, 88, 247-250.

Dramis, F., Sorriso-Valvo, M., 1994. Deep-seated gravitational slope deformations, related landslides and tectonics. Engineering Geology, 38, 231-2.

Duffield, W.A., Stieltjes, L., Varet, J., 1982. Huge landslide blocks in the growth of Piton de la Fournaise, La Reunion, and Kilauea, Hawaii. Journal of Volcanology and Geothermal Research, 12, 147-160.

Elsworth, D., Voight, B., 1995. Dike intrusion as a trigger for large earthquakes and the failure of volcano flanks. Journal of Geophysical Research, 100, 6005-6024.

Elsworth, D., Day, S.J., 1999. Flank collapse triggered by intrusion: the Canarian and Cape Verde Archipelagos. Journal of Volcanology and Geothermal Research, 94, 323-340.

Fekeč, J., Mahút, P., Novosad, P., 1970. Inžiniersko-geologický prieskum vrstevných zosuvov v zátopnej oblasti priehrady Šance (in Slovak). Mineralia Slovaca 2, 269-282.

Fúster, J.M., Hernán, F., Cendrero, A., Coello, J., Cantagrel, J. M., Ancochea, E., Ibarrola, E., 1993. Geocronología de la isla de El Hierro (Islas Canarias). Boletín de la Real Sociedad Española de Historia Natural, (Geología), 88, 86-97.

Gabler, R., Peterson, J., Trapasso, L., Sack, D., 2008. Physical geography. Cengage learning, Canada, p. 672.

Gee, M.J.R., Watts, A.B., Masson, D.G., Mitchel, N.C., 2001. Landslides and the evolution of El Hierro in the Canary Islands. Marine Geology, 177, 271-293.

GRAFCAN 2009. Topographical Map at 1/5.000 scale of the Canary Islands. Cartográfica De Canarias. Environmental Department of the Canarian Government. Gran Canaria.

Gudmundsson, A., 2012. Strengths and strain energies of volcanic edifices: implications for eruptions, collapse calderas, and landslides. Natural Hazards and Earth System Sciences, 12, 2241-2258, doi:10.5194/nhess-12-2241-2012

Guillou, H., Carracedo, J.C., Pérez-Torrado, F.J., Rodríguez Badiola, E., 1996. K-Ar ages and magnetic stratigraphy of a hotspot-induced, fast grown oceanic island: El Hierro, Canary Islands. Journal of Volcanology and Geothermal Research, 73, 141-155.

Günther, A., 2003. SLOPEMAP: programs for automated mapping of geometrical and kinematical properties of hard rock hill slopes. Computers and Geosciences 29, 865-875.

Horton, R. E., 1945. Erosional development of streams and their drainage basins: A hydrophysical approach to quantitative morphology. Bulletin of Geological Society of America, 56, 275-370.

Howard, A. D., 1967. Drainage analysis in geologic interpretation: A summation. Bulletin of American Association of Petroleum Geology, 51, 2246-2259.

Hunt, J. E., Wynn, R.B., Masson, D.G, Talling, P.J., Teagle, D.A.H., 2011. Sedimentological and geochemical evidence for multistage failure of volcanic island landslides: A case study from Icod landslide on north Tenerife, Canary Islands. Geochemistry Geophysics Geosystems, 12, 36.

Hürlimann, M., Garcia-Piera, J.O., Ledesma, A., 2000. Causes and mobility of large volcanic landslides: application to Tenerife, Canary Islands. Journal of Volcanology and Geothermal Research 103, 121-134.

Hürlimann, M., A. Ledesma, Martí, J., 2001. Characterisation of a volcanic residual soil and its implications for large landslide phenomena: application to Tenerife, Canary Islands. Engineering Geology, 59, 115-132.

Hürlimann, M., Martí, J., Ledesman, A., 2004. Morphological and geological aspects related to large slope failures on oceanic islands, the huge La Orotava landslides on Tenerife, Canary Islands. Geomorphology, 62, 143-158.

Husain, M., 2008. Geography of India. Tata McGraw-Hill, New Delhi.

IGME, 2008. Plan geode de cartografía Geológica continua, Instituto Geológico y Minero de España. Cartografía digital. Available online at: http://cuarzo.igme.es/sigeco/.

IGME, 2010ª. Plan MAGNA de cartografía geológica de España a escala 1:25.000. Isla de El Hierro. Hoja 1105-II, Valverde. Mapa geológico, mapa geomorfológico y memoria.

IGME, 2010b. Mapa Geológico de España, Escala 1:25.000. Isla de El Hierro. Hoja 1105-III, Sabinosa.

Imre, B., Alig, C., Schönenberger, I., Springman, S. M., Hermann, S., 2009. Morphology and kinematic of a very large, deep-seated structural rock slide located in the Fusch Valley, Eastern Alps, Austria. Geomorphology, 112, 277-294.

Jaboyedoff, M., Couture, R., Locat, P., 2009. Structural analysis of Turtle Mountain (Alberta) using digital elevation model: Toward a progressive failure. Geomorphology, 103, 5-16.

Jarman, D., Calvet, M., Corominas, J., Delmas, M., Gunnel, Y., 2014. Large-scale rock slope failures in the Eastern Pyrenees: identifying a sparse but significant population in

paraglacial and parafluvial contexts. Geografiska Annaler: Series A, Physical Geography, 96, 357–391, doi:10.1111/geoa.12060

Klimeš, J., Baroň, I., Pánek, T., Kosačík, T., Burda, J., Kresta, F., Hradecký J., 2009a. Investigation of recent catastrophic landslides in the flysch belt of Outer Western Carpathians (Czech Republic): progress towards better hazard assessment. Natural Hazards and Earth System Sciences, 9, 119-128.

Klimeš, J., Vilímek, V., Omelka, M., 2009b. Implications of geomorphological research for recent and prehistoric avalanches and related hazards at Huascaran, Peru. Natural Hazards, 50, 193-209.

Klimeš, J., Rowberry, M.D., Blahůt, J., Briestenský, M., Hartvich, F., Košťák, B., Rybář, J., Stemberk, J., Štěpančíkova, P., 2012. The monitoring of slow-moving landslides and assessment of stabilisation measures using an optical-mechanical crack gauge. Landslides, 9, 407-415.

Košťák, B., 2006. Deformation effects in rock massifs and their long-term monitoring. Quaternary Journal of Engineering Geology and Hydrogeology, 39, 249-258.

Krastel, S., Schmincke, H., Jacobs, C.L., Rihm, R., Le Bas, T.P., Alibés, B., 2001. Submarine landslides around the Canary Islands. Journal of Geophysical Research, 106, 3977-3997, doi: 10.1029/2000JB900413.

Křížek, M., Kusák, M., 2014. Variability of the morphometric characteristics of valley networks caused by variations in a scale. AUC Geographica, 1, 33-42.

Labazuy, P., 1996. Recurrent landslides events on the submarine flank of Piton de la Fournaise volcano (Reunion Island). In: Mc Guire, W.J., Jones, A.P., Neuberg (Eds.), Volcano instability on the earth and other planets. Journal of the Geological Society of London, 110, 295-306.

Longpré, M.A., Chadwick, J.P., Wijbrans, J., Iping, R., 2011. Age of the El Golfo debris

avalanche, El Hierro (Canary Islands): New constraints from laser and furnace 40Ar/39Ar dating. Journal of Volcanology and Geothermal Research, 203, 76-80.

Lo Giudice, E., Rasa, R., 1992. Very shallow earthquakes and brittle deformation in active volcanic areas. The Etnean region as an example. Tectonophysics, 202, 257-268.

López, C., Blanco, M. J., Abella, R., Brenes, B., Cabrera-Rodríguez, V. M., Casas, B., Domínguez-Cerdeña, I., Felpeto, A., Fernández de Villalta, M., Del Fresno, C., García, O., García-Arias, M. J., García-Canada, L., Gomis-Moreno, A., González-Alonso, E., Guzmán-Pérez, J., Iribarren, I., López-Díaz, R., Luengo-Oroz, N., Meletlidis, S., Moreno, M., Moure, D., Pereda de Pablo, J., Rodero, C., Romero, E., Sainz-Maza, S., Sentre-Domingo, M. A., Torres, P. A., Trigo, P., and Villasante-Marcos, M., 2012. Monitoring the unrest of El Hierro (Canary Islands) before the onset of the 2011 Submarine Eruption, Geophysical Research Letters, 39,L13303, doi:10.1029/2012GL051846

Martín-Ramos, J.D., 2004. Using XPowder®, a sofware package for powder X-ray diffraction analysis. D.L.GR-1001/04. Spain.

Martí, J., Hurlimann, M., Ablay, G. J., Gudmundsson, A., 1997. Vertical and lateral collapses on Tenerife (Canary Islands) and other volcanic ocean islands. Geology, 25, 879-882.

Marti, X., Rowberry, M.D., Blahůt, J., 2013. A MATLAB® code for counting the moiré interference fringes recorded by the optical-mechanical crack gauge TM-71. Computers and Geosciences, 52, 164-167.

Masson, D.G., 1996. Catastrophic collapse of the volcanic island of Hierro 15 ka ago and the history of landslides in the Canary lslands. Geology, 24, 231-234.

Masson, D.G., Watts, A.B., Gee, M.J.R., Urgeles, R., Mitchel, N.C., Le Bas, T.P., Canals, M., 2002. Slope failures on the flanks of the western Canary Islands. Earth-Science Reviews, 57, 1-35.

Masson, D. G., Le Bas, T., Grevemeyer, I., Weinrebe, W., 2008. Flank collapse and large-scale landsliding in the Cape Verde Islands, off West African, Geochemistry, Geophysics and Geosystems, 9, Q07015, doi:10.1029/2008GC001983.

Meentemeyer, R.K., Moody, A., 2000. Automated mapping of conformity between topographic and geological surfaces. Computers and Geosciences, 26, 815 – 829.

Mitchell, N.C., Quartau, R., Madeira, J., 2012. Assessing landslide movements in volcanic islands using near-shore marine geophysical data: south Pico island, Azores. Bulletin of Volcanology 74 , 483-496.

Moon, V., Simpson, C.H.J., 2002. Large scale wasting in ancient volcanic materials. Engineering Geology, 64, 41-64.

Moore, J.G., Normark, W.R., Holcomb, R.T., 1994. Giant Hawaiian landslides. Annual Review of Earth and Planetary Sciences, 22, 119-144.

Moore, J.G., Chadwick, W.W. Jr., 1995. Offshore geology of Mauna Loa and adjacent areas, Hawaii. In: Rhodes, J.M., Lockwood, J.P. (Eds.), Geophysical Monograph 92, Mauna Loa Revealed: structure, composition, history, and hazards. American Geophysical Union, Washington, D.C., 21-44.

Moro, M., Saroli, M., Salvi, S., Stramondo, S., Doumaz, F., 2007. The relationship between seismic deformation and deep–seated gravitational movements during the 1997 Umbria–Marche (Central Italy) earthquakes. Geomorphology, 89, 297-307.

Novotný, J., Klimeš, J., 2014. Grain size distribution of soils within the Cordillera Blanca, Peru: an indicator of basic mechanical properties for slope stability evaluation. Journal of Mountain Science, 11, 563-577.

Pánek, T., Táborík, P., Klimeš, J., Komárková, V., Hradecký, J., Šťastný, M., 2011. Deep-seated gravitational slope deformations in the highest parts of the Czech Flysch Carpathians: evolutionary model based on kinematic analysis, electrical imaging and trenching. Geomorphology, 129, 92-112.

Pararas-Carayannis, G., 2002. Evaluation of the threat of mega tsunami generation from postulated massive slope failures of island volcanoes on La Palma, Canary Islands, and on the Island of Hawaii. Science of Tsunami Hazards, 20, 251-277.

Pradhan, B., Singh, R. P., Buchroither, M. F., 2009. Estimation of stress and its use in evaluation of landslide prone regions using remote sensing data. Advanced in Space Research, 37, 698-709.

Price, L. W., 1986. Mountains and Man: A Study of Process and Environment. University of California Press, USA.

Rodríguez-Losada, J.A., Hernández-Gutiérrez, L.E., Olalla, C., Perucho, A., Serrano, A., del Potro, 2007. The volcanic rocks of the Canary Islands, geotechnical properties. Proceedings of the International Workshop on Volcanic Rocks, Ponta Delgada (San Miguel, Azores), pp. 53-57.

Rodríguez-Losada, J.A., Hernández-Gutiérrez, L.E., Olalla, C., Perucho, A., Serrano, A., Eff-Darwich, A., 2009. Geomechanical parameters of intact rocks and rock masses from the Canary Islands: Implications on their flank stability. Journal of Volcanology and Geothermal Research, 182, 67-75.

Santangelo, M., Marchesini, I., Cardinali, M., Fiorucci, F., Rossi, M., Bucci, F., Guzzetti, F., 2015. A method for the assessment of the influence of bedding on landslide abundance and types. Landslides, 2, 295-309, doi: 10.1007/s10346-014-0485-x.

Sassa, K., Dang, K., He, B., Takara, K., Inoue, K., Nagai, O., 2014. A new high-stress undrained ring-shear apparatus and its application to the 1792 Unzen–Mayuyama megaslide in Japan. Landslides, 11, 827-842.

Seta, D.M., Marotta, E., Orsi, G., de Vita, S., Sansivero, F., Fredi, P., 2011. Slope instability induced by volcano-tectonics as an additional source of hazard in active volcanic areas: the case of Ischia Island (Italy). Bulletin of Volcanology, 74, 79-106, doi: 10.1007/s00445-011-0501-0.

Schmincke, H.U., Sumita, M., 2010. Geological evolution of the Canary Islands: Koblenz, Germany, Görres-Verlag.

Snyder, R.L., Bish, D.L., 1989. Quantitative analysis. In: Bish, D.L., Post, J.E., (Eds.), Modern Powder Diffraction Reviews in Mineralogy 20. Mineralogical Society of America, pp. 101-143.

Terzaghi, K., 1950. Mechanism of landslides. Memoirs of Geological Society of America, Berkey, pp. 89-123.

Tibaldi, A., 2001. Multiple sector collapses at Stromboli, Italy: how they work. Bulletin of Volcanology, 63, 112-125.

Tibaldi, A., 2004. Major changes in volcano behaviour after a sector collapse: insights from Stromboli, Italy. Terra Nova, 16, 1, 2–8, doi: 10.1046/j.1365-3121.2003.00517.x.

Urgeles, R., Canals, M., Baraza, J., Alonso, B., 1996. The submarine “El Golfo” debris avalanche and the Canary debris flow, West Hierro Island: the last major slides in the Canary archipelago. Geogaceta, 20, 390-393.

Urgeles, R., Canals, M., Baraza, J., Alonso, B., Masson, D.G., 1997. The most recent megaslides on the Canary Islands: the El Golfo Debris Avalanche and the Canary Debris Flow, west El Hierro Island. Journal of Geophysical Research, 102, 20305-20323.

Voight, B., 2000. Structural stability of andesite volcanoes and lava domes. Philosophical Transactions of the Royal Society of London, 358, 1663-1703.

Vilímek, V., Zvelebil, J., Klimeš, J., Patzelt, Z., Astete, F., Kachlík, V., Hartvich, F., 2007. Geomorphological research of large-scale slope instability at Machu Picchu, Peru. Geomorphology, 89, 241-257.

Whelan, F., Kelletat, D. 2003. Submarine slides on volcanic islands - a source for mega-tsunamis in the Quaternary. Progress in Physical Geography, 27, 198-216.

Yepes, J.T., Sánchez, N., Rodrígues-Peces, Galindo, I., del Potro, R., 2013a. Geomorphologic evidence of great flank collapses in the northwestern Grand Canaria (Canary Islands, Spain). In: Margottini, C., Canuti, P., Sassa, K., (Eds.), Landslide Science and Practice, 7, Springer, 217-221, doi: 10.1007/978-3-642-31313-4_28

Yepes, J.T., Sánchez, N., Rodrígues-Peces, Galindo, I., del Potro, R., 2013b. Geomorphologic evidence of flank instabilities in the eastern sector of the Tejeda Volcano (Canary Islands, Spain) during the Quaternary. In: Margottini, C., Canuti, P., Sassa, K. (Eds.), Landslide Science and Practice, 7, Springer, 65-72, doi: 10.1007/978-3-642-31313-4_9.

Zâvoianu, I., Herișanu, G., Cruceru, N., 2009. Classification systems for the hydrographical network. Forum Geografic, 8, 58-63.

Zorzi, L., Massironi, M., Surian, N., Genevois, R., Floris, M., 2014. How multiple foliations may control large gravitational phenomena: A case study from the Cismo Valley, Eastern Alps, Italy. Geomorphology, 207, 149-160.

Table 1 Basic mechanical properties of the potential slide plane infill material from the Tijirote water gallery. S – Sand, M – Mud, C - Clay, LL - Liquid Limit, PL - Plastic Limit, PI - Plasticity Index, ρ_s - Unit weight.

Site	S (%)	M (%)	C (%)	LL (%)	PL (%)	PI	ρ_s (g/m^3)
Tijirote gallery	24.9	62.5	12.6	28.5	20.91	7.9	2.85

Table 2 Morphometric characteristics of the valley network around the SAL. Characteristics written in bold are unique within the El Hierro Island.

Parts of San Andrés	Valley order	Number of valleys	Total length of valleys [m]	Valley networks´ density [$m\ m^{-2}$]	Valley junction angles	Valley network type
Tiñor	I. order	33	33,660	0.0055	46°01´12´´	dendritic
	II. order	93	39,226.28			
	III. order	80	23,750.1			
	IV. order	21	3,998.36			
	V. order	1	224.56			
SA North	I. order	23	27,759.4	0.0055	76°21´	rectangular
	II. order	60	22,688.76			
	III. order	31	6,253.87			
	IV. order	10	453.31			
	V. order	1	197.16			
SA South	I. order	21	33,067.56	0.0076	21°57´	parallel
	II. order	75	34,042.32			

	III. order	36	10,460.45			
	IV. order	12	957.39			
	V. order	-	-			
Punto Limpio	I. order	6	6,281.73	0.0072	35°08´24´´	parallel
	II. order	22	12,806.35			
	III. order	25	8,938.42			
	IV. order	9	1,975.86			
	V. order	1	284.01			

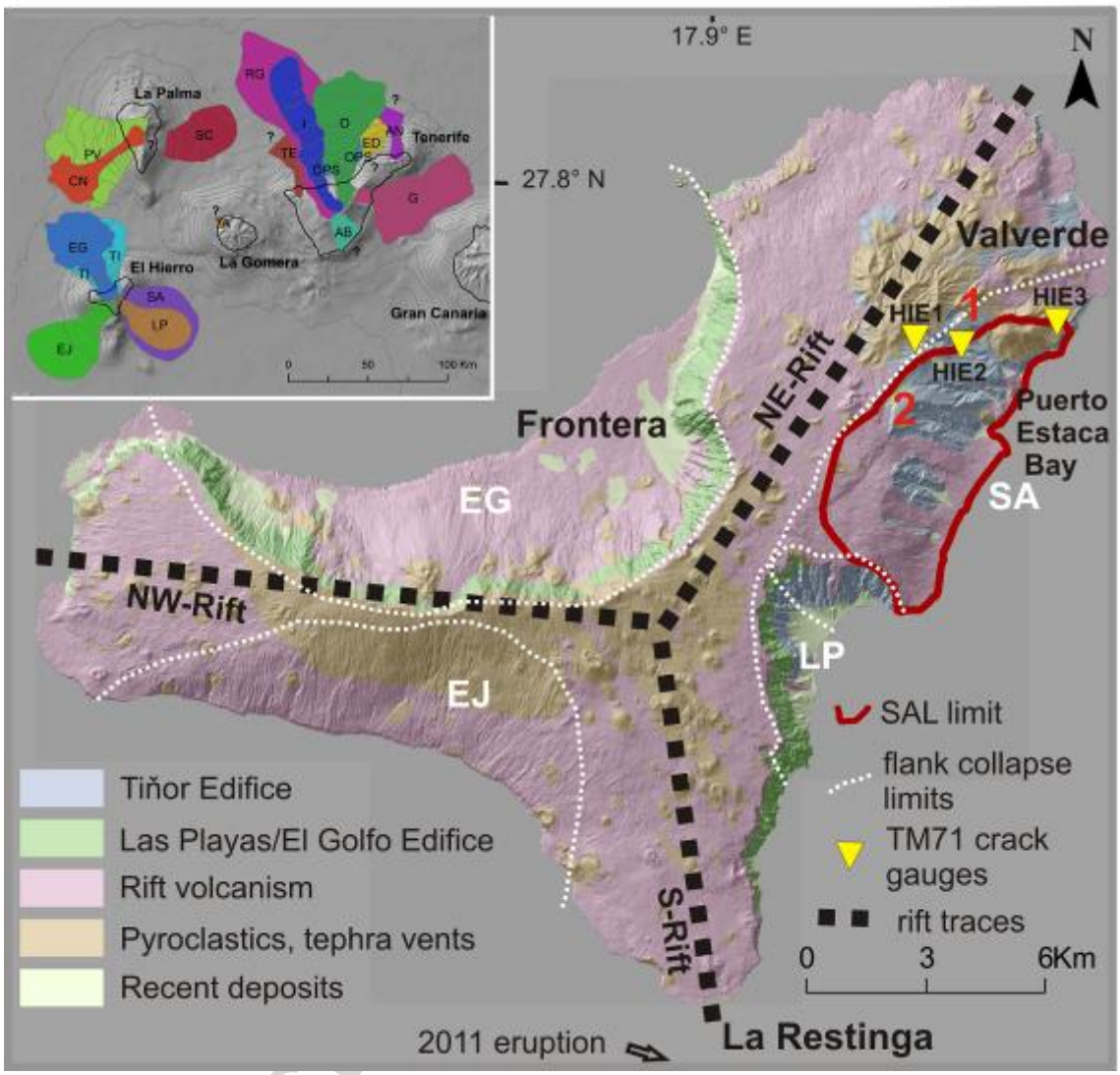

Fig. 1 Generalized geological map of the island of El Hierro (data from IGME, 2008) showing the limits of previously identified large flank collapses: EG - El Golfo, EJ - El Julan, LP - Las Playas I, SA - San Andrés, also called as Las Playas II, 1 and 2 indicate the location of the Tijirote gallery and the Balón ravine, respectively. The inset figure shows the main landslide deposits on the Western Canary Islands based on Gee (2001), Carracedo et al. (2001), Masson et al. (2002), Acosta et al. (2003), Hürlimann et al. (2004), Dávila et al. (2011), Longprè et al. (2011). TI – Tiñor, SC - Santa Cruz, CN - Cumbre Nueva, PV - Playa de la Veta, I – Icod, O - La Ortova, RG - Roques de García, AB - Abona, G – Güímar, OPS - Old post-shield, AN – Anaga, TE – Teno, ED - East Dorsal.

Fig. 2 Location and device characteristics of the monitored sites with the TM-71 crack gauge on the island of El Hierro. Photograph of the HIE1 shows the setting of the automated reading device installed on the TM-71 crack gauge. It consists of computer (white box on the floor), web cameras (on the crack gauge) and environmental monitoring station (dark box with large display on the PC, measuring air temperature/pressure and humidity). Electricity is supplied by car battery.

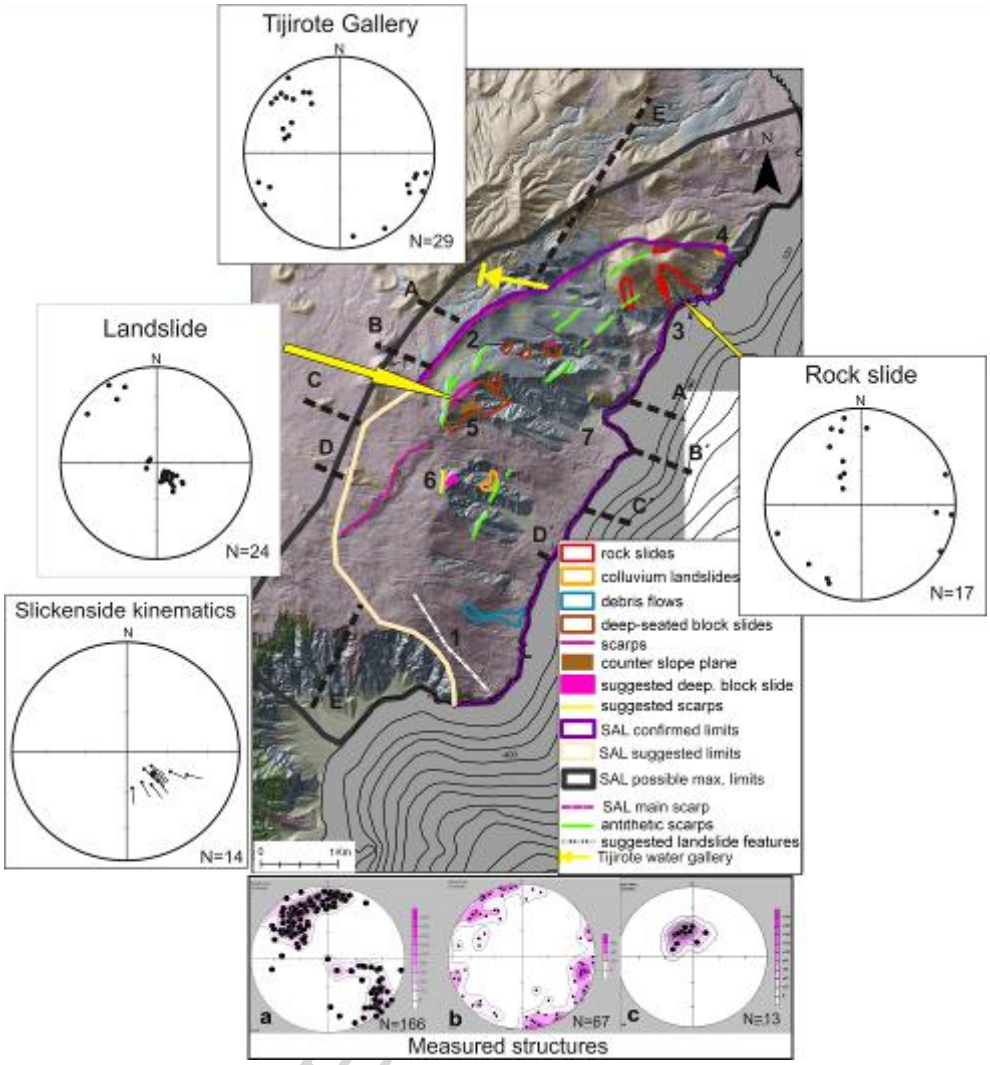

Fig. 3 Landslide inventory map with topographic profile traces (simplified geology is shown on colour figure only, for its legend see Fig. 1). 1 gully, 2 - trench below main scarp of the SAL, 3 - Port of Estaca, 4 - colluvial landslide, 5 - deep-seated block slide, 6 - suggested deep-seated block slide, 7 - Balón ravine. Contour lines below sea level have an interval of 100 m. The spatial distribution of structural measurements within specific landforms inside the SAL is shown on the inset images. N - number of measurements shown, 'Landslide' - shows detailed measurements inside the body of deep-seated block slide, 'Tijirote gallery' - shows structural measurements inside the gallery, 'Rock slide' - measurements mainly from the scarp area of larger and deeper landslide which involved pyroclastics. Inset figure entitled 'Measured Structures' shows all structural measurements within the SAL classified into three

classes: a - SAL scarps planes, b - fractures, c - bedding planes, which represent surfaces sub-parallel with the slope surface with a variety of origin.

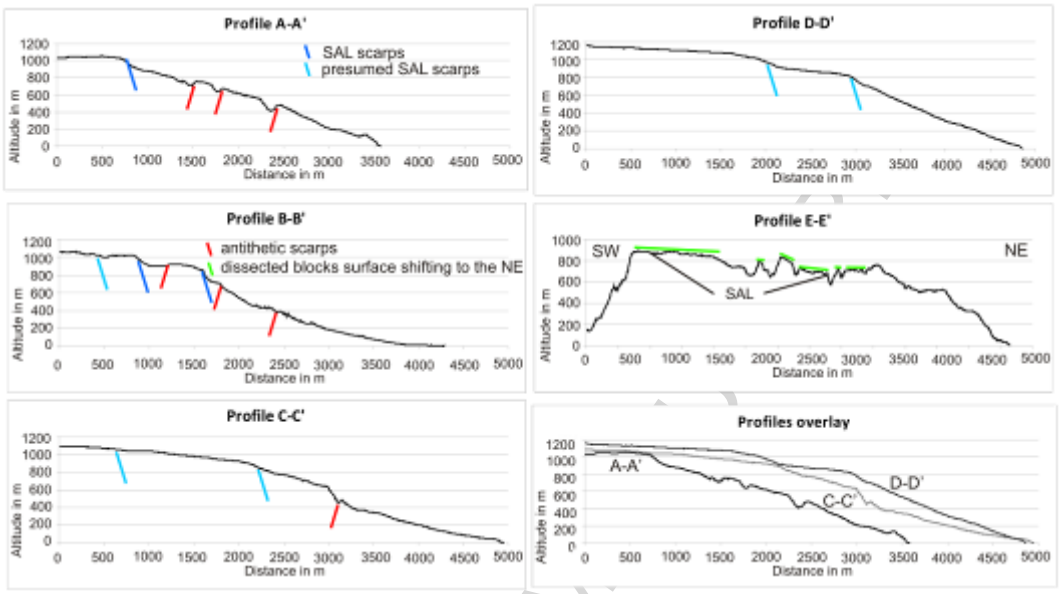

Fig. 4 Topographic profiles where different morphological features such as scarps, antithetic scarps, shallow inclined planes or trenches, related to the SAL are shown. Traces of the topographic profiles are shown in Fig. 3.

Fig. 5 Results of regional kinematic testing of landslide occurrence conditions on the subaerial part of the SAL (black solid line) showing areas susceptible to sliding under two specified conditions: 1 - areas susceptible to planar failure constrained by spatially distributed structural measurements (DSM) of the SAL slip planes and recent DEM with angle of internal friction ranging from 0° to 25°. 2 - areas susceptible to planar or wedge failure mechanism on the hypothetical basal sliding plane with angle of internal friction lower than 7°. Contours of the secondary landslides are shown for reference.

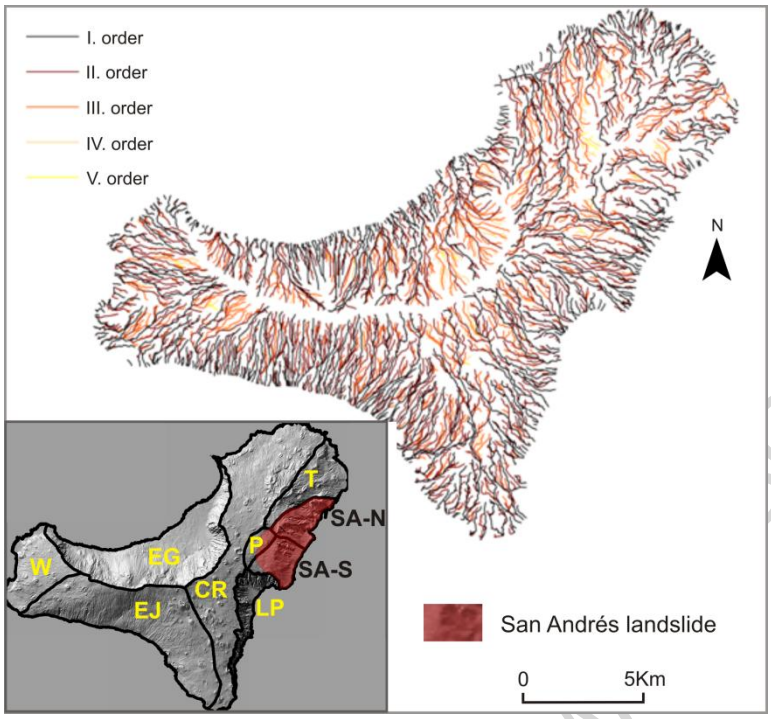

Fig. 6 Valley network up to V order. Inset shows division of the island into separate areas where valley network was characterized (W – West, EG - El Golfo, EJ - El Julan, CR - Central Rift, LP - Las Playas, P - Punto Limpio, T – Tiñor, SA-S - San Andrés South, SA-N - San Andrés North.

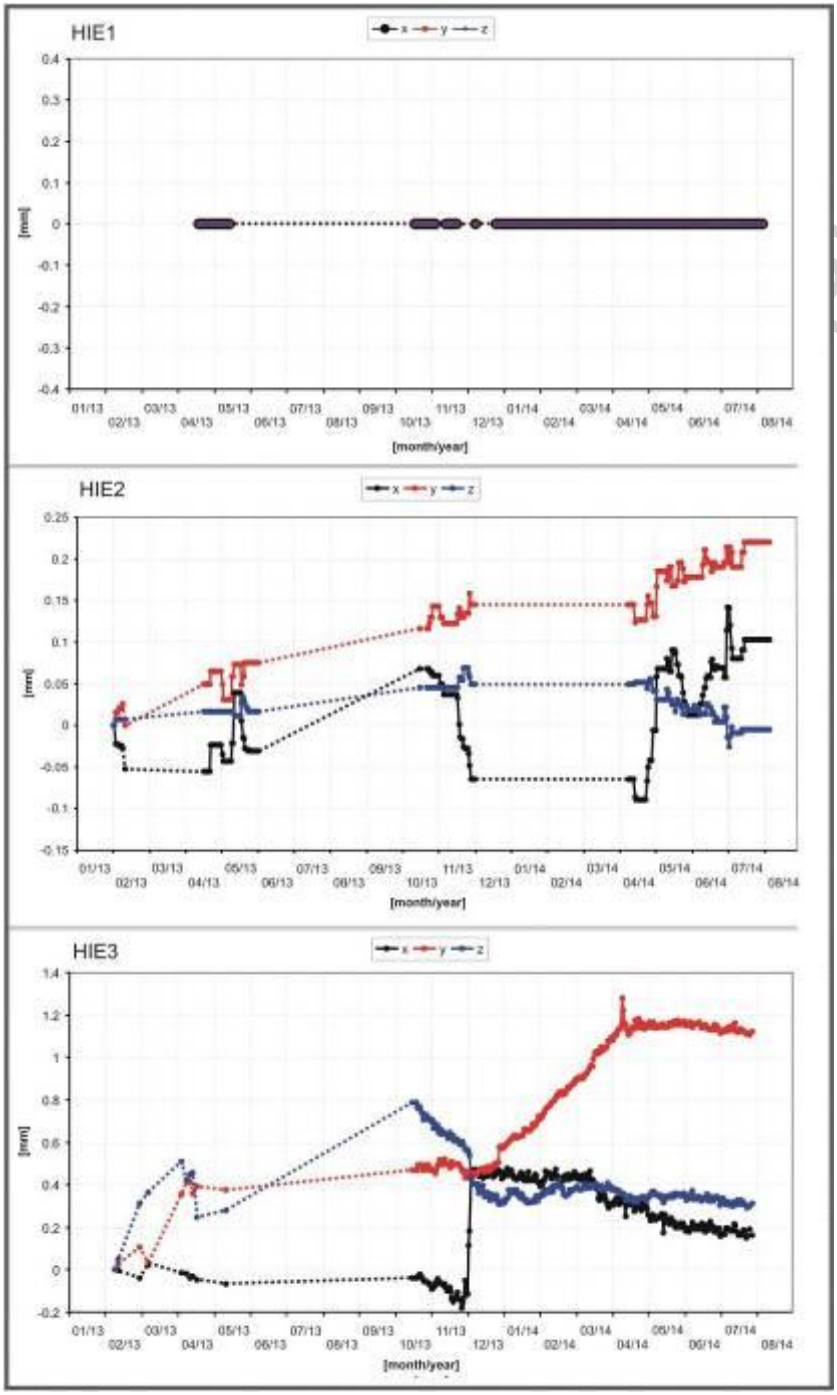

Fig. 7 Results of the TM-71 crack gauge monitoring. HIE1 does not show movements at all during the monitoring period unlike HIE2 and HIE3. Horizontal movements (x and y) dominate over vertical displacements. Positive x values show compression, positive y values indicate sinistral strike slip, and positive z values represent movements of the downslope block in the upslope direction.

Highlights:

- A long-term, automated landslide movement monitoring system was installed
- A year-long monitoring shows creep activity on the landslide scarps
- Environmental conditions remain favourable for possible future landslide activity
- Morphological evidence suggests that the landslide has recently developed
- The newly obtained data suggest possible future movement at accelerated velocities